Electronic Supplementary Information for

Ionic Conductivity of Mesoporous Electrolytes with a High Density of Pyridinium Groups within their Framework

M. Waki,[*a,b‡] S. Fujita[b] and S. Inagaki[a,b,c]

[a] Toyota Central R&D Labs., Inc., Nagatute, Aichi 480-1192, Japan.
[b] Core Research for Evolutional Science and Technology (CREST), Japan Science and Technology Agency (JST), Kawaguchi, Saitama 332-0012, Japan.
[c] Advanced Catalytic Transformation Program for Carbon Utilization (ACT-C), Japan Science and Technology Agency (JST), Kawaguchi, Saitama 332-0012, Japan.
‡Present address: Graduate School of Medicine, Dentistry and Pharmaceutical Sciences, Okayama University, 1-1-1 Tsushima-naka, Kita-ku, Okayama 700-8530, Japan.

Experiment

General: Commercially available reagents and solvents were used without further purification. ^{29}Si dipolar decoupling (DD) and ^{13}C cross polarization (CP)-magic angle spinning (MAS) NMR spectroscopy measurements were respectively performed at 79.49 and 100.6 MHz at a sample spinning frequency of 4 kHz using a Bruker Avance 400 spectrometer with a 7 mm zirconia rotor. ^{29}Si DD-MAS NMR measurements were conducted with a repetition delay of 80 s and a pulse width of 4.5 μs. The ^{13}C CP-MAS NMR measurements were conducted with a repetition delay of 5 s, a contact time of 1.75 ms, and a pulse width of 4.5 μs (^{1}H 90° pulse). Chemical shifts were referenced to tetramethylsilane and glycine for ^{29}Si and ^{13}C NMR, respectively. X-ray diffraction (XRD) profiles were recorded on a Rigaku RINT-TTR diffractometer using Cu Kα radiation (50 kV, 300 mV). Nitrogen adsorption and desorption isotherms were measured using a Yuasa Nova3000e sorptometer. Brunauer-Emmett-Teller (BET) surface areas were calculated from the linear sections of BET plots (P/P_0 = 0.1–0.2). Pore-size distributions were calculated using the density functional theory (DFT) method (DFT kernel: N_2 at 77 K on silica, cylindrical pores, nonlinear DFT (NLDFT) equilibrium model) from adsorption branch of the isotherm. Pore volumes were estimated by the t-plot method. IR spectra were collected on a Thermo Fisher Scientific Nicolet Avatar-360 FT-IR spectrometer using an attenuated total reflection (ATR) attachment. UV/vis absorption and fluorescence emission spectra were obtained using Jasco V-670 and FP-6500 spectrometers, respectively.

Synthesis

v-Py-PMO: The v-Py-PMO material was prepared according to the method previously reported in the literature.[33]

Divinylbenzene-PMO: The divinylbenzene-PMO material was prepared according to the method previously reported in the literature.[35,36] Obtained PMO herein has the surface area (753 m^2 g^{-1}) and large pore volume (0.476 cm^3 g^{-1}).

PyH^+-PMO: 2,5-Bis[(E)-2-(triethoxysilyl)vinyl]pyridine (0.55 g, 1.2 mmol) was added to a mixture of sodium dodecylsulfate (SDS) (0.50 g) and a 12 N hydrochloride aqueous solution (0.25 mL) in distilled water (30 mL) under vigorous stirring at room temperature. The suspension was stirred for additional 24 h. The suspension was heated at 96 ºC for 48 h under a static condition. Then, the resulting precipitate was filtered and washed with distilled water, affording as-made PMO. The as-made materials were dried at 100 ºC under vacuum. The surfactant was removed by liquid extraction of the as-made materials (0.34 g) in EtOH (49 mL) with concentrated HCl (1.3 g) at 60 ºC for 16 h.

Ionic conductivity measurement

The ion conductivity was measured using electrochemical impedance spectroscopy with a Hioki 3532-50 LCR Hitester. The frequency range was 50 Hz to 5 MHz with an oscillating voltage of 0.1 V. Prior to the measurement, the mesoporous electrolyte powder was pressed into small pellets (2 cm diameter and 200 μm thick) and inserted between Pt electrodes. The conductivity was calculated according to the formula $\sigma = (1/R)/(L/A)$, where R is the resistance, L the thickness of the electrolyte between the electrodes, and A the cross-sectional contact area of the electrodes. Measurements were conducted under fully saturated humidification (100% relative humidity (RH)) at the desired temperature.

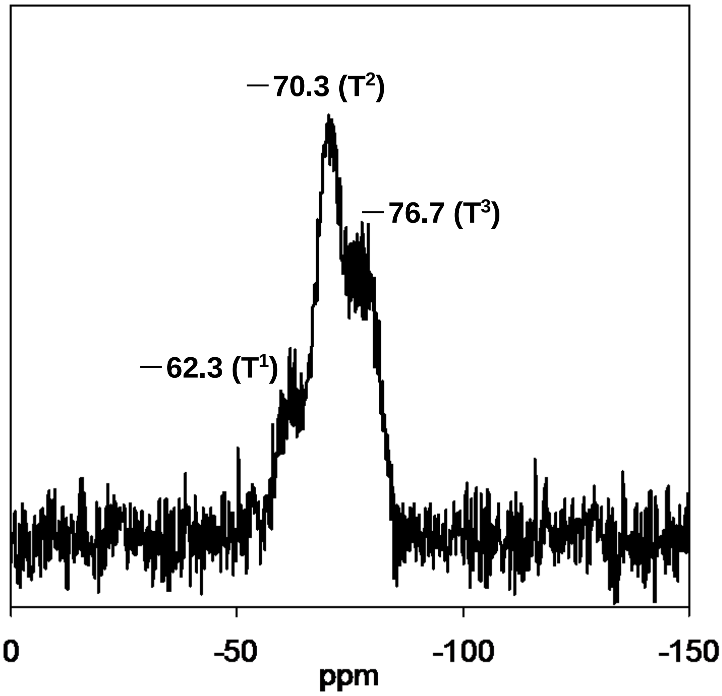

Fig. S1 ^{29}Si MAS NMR spectrum of PyH^{+}-PMO.

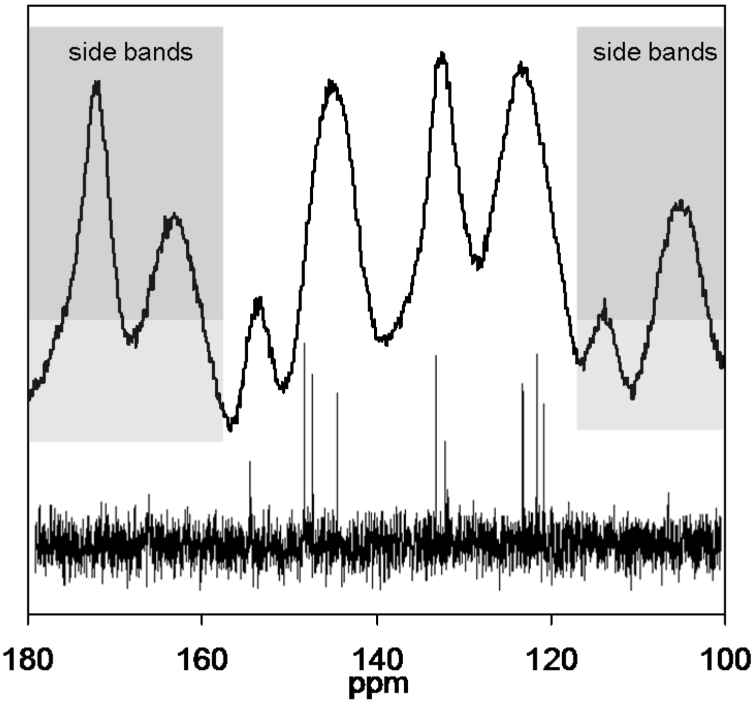

Fig. S2 ^{13}C CP-MAS NMR spectrum of PyH^{+}-PMO and ^{13}C NMR spectrum of pyridine precursor in CDCl$_3$.

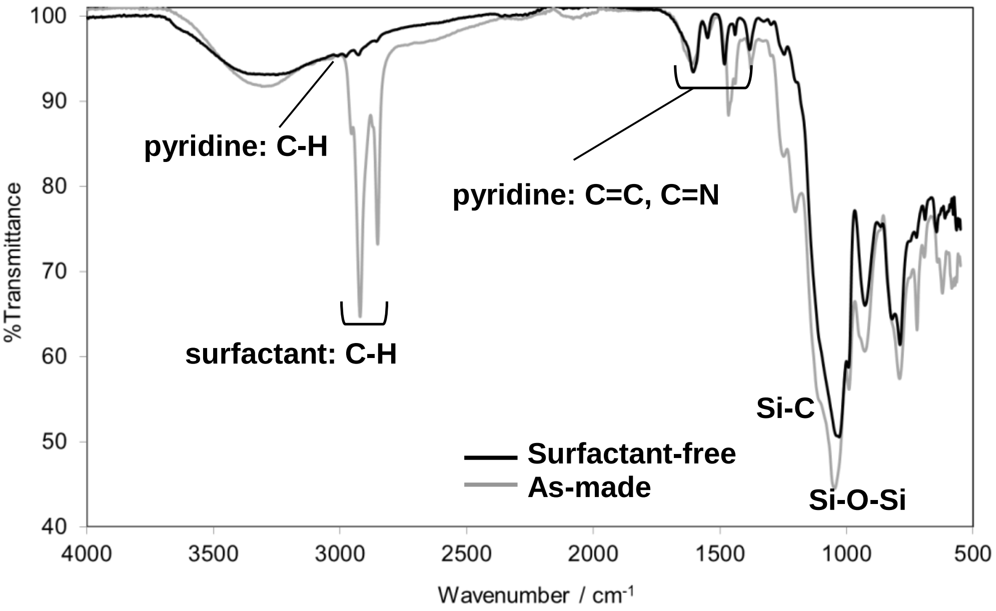

Fig. S3 IR spectra of PyH$^+$-PMO before and after an extraction of the surfactant. The bands are assigned as follows: ν(SiO-H) at 3371 cm^{-1}, ν(C=C)aromatic at 1587, 1533, 1475, 1390 and 1354 cm^{-1}, ν(C-Si) at 1151 cm^{-1}, and ν(Si-O) at 1032 cm^{-1}. In spectrum of as-made sample, characteristic peaks were observed at 2850 and 2920 cm^{-1}, which were assignable to the C-H stretching modes of the alkyl chain of the surfactant. Disappearance of the bands confirms removal of the surfactant by solvent extraction using a HCl–ethanol solution.

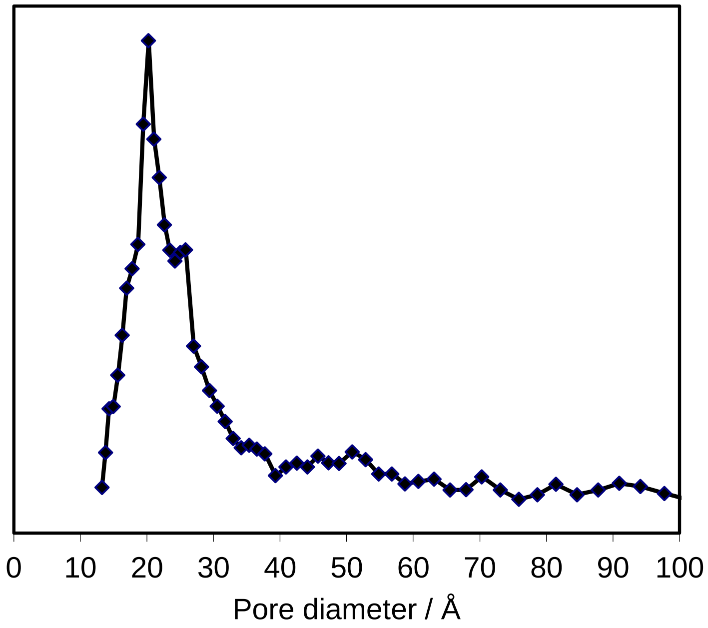

Fig.S4 Pore size distribution of PyH$^+$-PMO.